JOURNAL OF MECHANICS OF CONTINUA AND MATHEMATICAL SCIENCES
www.journalimcms.org

ISSN (Online) : 2454 -7190 Vol.-19, No.-11, November (2024) pp 173 - 190 ISSN (Print) 0973-8975

DEVELOPMENT AND EVALUATION OF A VERSATILE CONTROL SYSTEM IN AN ADAPTABLE MULTI-LEGGED ROBOT USING A MODIFIED PEAUCELLIER-LIPKIN MECHANISM

Papatla Rajesh[1], Rega Rajendra[2], Ponugoti Gangadhara Rao[3]

[1] Department of Mechanical Engineering, OUCE Hyderabad, 500007 Telangana, India.

[1] Department of Mechanical Engineering, SIR C.R.Reddy College of Engineering,534007 Eluru, Andhra Pradesh, India.

[2] Department of Mechanical Engineering, OUCE, Hyderabad, 500007 Telangana, India.

[3] Department of Mechanical Engineering, Aditya College of Engineering and Technology, 533437 Surampallem, Andhra Pradesh, India.

Email : rajeshbabu93@gmail.com, regaraj@gmail.com, audibalav@gmail.com

Corresponding Author: **Papatla Rajesh**

https://doi.org/10.26782/jmcms.2024.11.00012

(Received: July 26, 2024; Revised: October 19, 2024; Accepted: November 02, 2024)

Abstract

The present work in bio-inspired robotics explores the design and implementation of a novel-legged robotic system featuring a modified Peaucellier-Lipkin mechanism with three control points for a single degree of freedom. The emphasis is placed on the robot's adaptability to various walking gaits in different environments. The paper delves into the robot's design, construction, and control system, which includes the application of PID control for enhanced stability and efficiency in mimicking biological locomotion. The primary aim is to demonstrate a robot capable of adjusting its form and function for diverse operational challenges, enhancing robotic mobility. The design also addresses repeatability issues, ensuring consistent performance across various tasks and conditions, contributing to the robot's reliability and practical applicability in real-world scenarios.

Keywords: Biological locomotion, Peaucellier-Lipkin mechanism, PID controller repeatability, Robotic mobility.

I. Introduction

Wheeled locomotion, effective on flat surfaces, often struggles on uneven terrain, prompting a shift towards leg-based robots that mimic the adaptive gait of animals. These robots are notable for their energy efficiency and obstacle navigation capabilities, as outlined in references [XIII], [XVIII], [XXV]. In this field, a significant

focus has been on single-degree-of-freedom mechanisms like the Klann linkage [XVI]. This mechanism is ideal for leg-based systems due to its simplicity and cost-effectiveness, enhancing adaptability and versatility in bio-inspired robotics for complex terrains. The authors in reference [XX] have made significant advancements in the Klann mechanism, a stable and energy-efficient variation of the Stephenson type III kinematic chain. This mechanism enhances quadruped robots' gait adaptability, offering an effective alternative to wheels. Jaichandar et al. [XI], [XII] and Sun and Zhao [XXI] further improved legged robotics by focusing on adaptable footprints and movement trajectories, as well as developing robots with morphing joints. Additionally, [XVII] and Vanitha U. et al. [XXIII] have expanded the functionality of spider bots through the Klann mechanism, increasing their maneuverability across different environments. Theo Jansen [X] created a mechanism that mimics animal walking, enhancing robot movement design. Ghassaei [VII] improved on this with more designs for crank-based legs. Bhavsar and team [II] analyzed an eight-legged robot using Jansen's design, providing new perspectives on robotic legs. Sutysadi and colleagues [XXII] also worked on crank-based legs and robot stability, using an H∞ controller to ensure stable movements in various conditions. Building on this foundation, Alexeev et al. [I] innovatively enhanced a walking robot using a modified Jansen linkage, concentrating on improving stability and efficiency. This development is crucial for the practical use of leg-based robots in various environments, marking a significant advancement towards more reliable and versatile robotic applications. Xi Chen et al. [III] also contributed by developing a multi-legged walking robot prototype, highlighting the role of servo motors in bio-inspired gait execution. Daniel Giesbrecht et al. [VIII] have focused on an 8-bar-legged walking mechanism to reduce energy consumption and increase walking distance. Advancing the developments in leg-based robotics, Shivamanappa et al. [V] introduced innovative single-degree-of-freedom, crank-driven walking leg mechanisms that surpass existing models in simplicity, efficiency, and adaptability. Given these advancements, it's clear that legged robots necessitate sophisticated control systems to deftly handle a variety of terrains. This has led to an evolution from basic proportional-integral-derivative (PID) control to more advanced soft computing techniques [XXIV], [XIV], which include practical PID applications in servomotors, microcontroller interfacing, and the optimization of metaheuristic algorithms [XIX], [VI]. As research progresses, optimized PID tuning and the integration of artificial intelligence, as outlined in reference [IX], [XV] promise to yield smarter, more energy-efficient control systems. These technological developments closely mirror the adaptability observed in legged robots, paving the way for robots capable of navigating diverse terrains with agility and efficiency. In advancing robotic control systems, S. Chwila [IV] has made significant contributions by enhancing robotic flexibility and sensor integration and by improving user interaction and real-time monitoring capabilities. These efforts are pushing the boundaries of what is achievable in modern robotics. The present work introduces an innovative leg mechanism for walking robots, designed to address repeatability issues across different gaits. It features a single-degree-of-freedom, crank-driven system utilizing a modified Peaucellier-Lipkin linkage in an eight-bar configuration. The design focuses on overcoming the constraints associated with traditional rotating cranks by adding control points at C and D (Fig. 1), thus enhancing adaptability and reducing the risk of failure. The mechanism's motion is analyzed both structurally and

functionally, with various configurations demonstrating improved reliability and adaptability. Performance is evaluated through the analysis of position, velocity, and acceleration, supported by simulations. An integrated PID control system continuously manages these points, ensuring precise monitoring and adjustment of each link movement. Additionally, by incorporating the stabilization and orientation sensor module into the robot's control system, the module can effectively monitor and mitigate vibrations in the robot's body, leading to a more stable and controlled movement. This process efficiently calculates joint displacements and ensures a smooth, consistent trajectory.

II. Background Theory

Legged robotics has emerged as a promising solution to the challenges wheeled systems face on irregular terrain. The pursuit of efficiency and adaptability has led to the creation of single-degree freedom mechanisms such as the Janson-Klann linkage, which draws inspiration from animal movement. These linkages use the straightforward and affordable Stephenson type III kinematic chain to provide stable and efficient motion, offering a practical substitute for conventional wheeled systems. With the integration of reconfigurable systems into legged robots, the Klann mechanism's adaptability to varying terrains is significantly enhanced. The collective efforts in the field have been directed towards improving the energy efficiency, reconfigurability, and stability of walking mechanisms. This has led to the exploration of control systems that evolve from basic PID control to the application of advanced soft computing techniques and AI integration for smarter, more energy-efficient solutions. This paper presents a cutting-edge leg mechanism that adopts a modified Peaucellier-Lipkin linkage within an eight-bar framework. By introducing additional control points and eschewing the constraints of traditional cranks, the mechanism showcases improved structural and functional motion, reliability, and adaptability across different configurations. The mechanism's performance, evaluated through detailed kinematic analysis and simulations, underscores its potential to provide smooth, consistent trajectories for legged robots operating in challenging environments.

III. Exploring A Modified Peaucellier-Lipkin Mechanism: Cad Design and Experimental Setup

In this section, we delve into the intricacies of computer-aided design (CAD) and the experimental setup of the modified Peaucellier-Lipkin mechanism. Our focus is on providing a detailed account of the design process using CAD-based tools, coupled with insights into the experimental framework that validates the functionality and adaptability of the modified mechanism. This dual perspective aims to offer a better understanding of both the theoretical underpinnings and the practical implementation of the innovative Peaucellier-Lipkin modification.

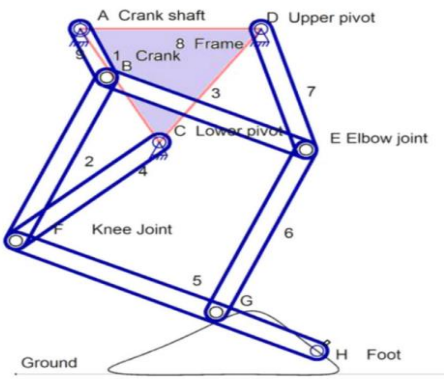

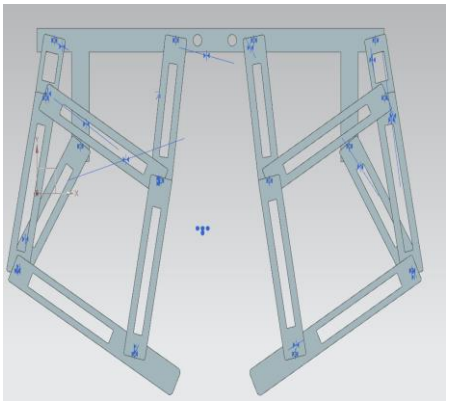

Fig 1. Peaucellier-Lipkin Mechanism. Ref [XVIII] **Fig 2.** Cad Modelled of Leg Using NX. 12.

Figure 1 depicts the primary walking mechanism, while Figure 2 was created using the NX modelling environment. The CAD model underwent virtual simulation in the motion environment to identify and rectify any mechanical failures. Once verified, it was transferred to the linkage mechanism design and simulator for motion and path-tracing tests.

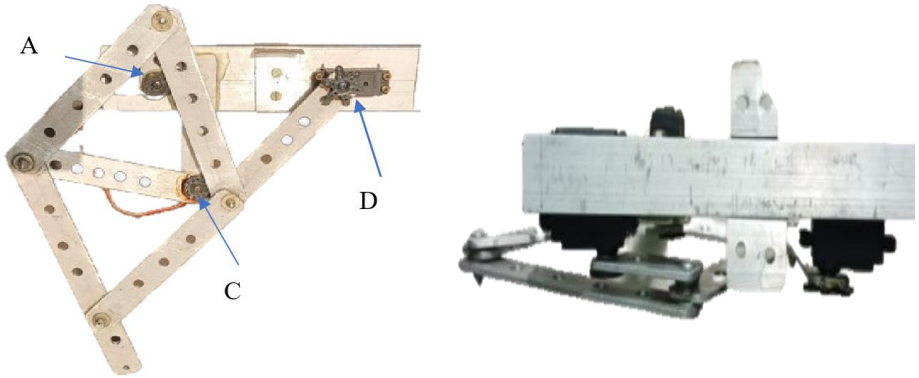

(a) (b)

Fig 3. Front and Top View of Reconfigurable Design.

Figure 3 shows a comprehensive upgrade to the Peaucellier-Lipkin mechanism, which includes both physical enhancements and virtual simulation aspects. The mechanism, which originally had only one motor controlling the origin joint, now features three advanced angular rotary actuators positioned at key joints of frame A, lower pivot C, and upper pivot D, respectively. These actuators provide precise movement control and are integral to the mechanism's improved adaptability and stability. This is carefully designed and simulated in linkage mechanism design software. In this simulation, each link is crafted with precision, and motors are strategically placed. The two motors driving the walking leg system can rotate in both directions, with a feedback system

correcting any deviations automatically. This simulation provides a clear picture of the mechanism's dynamics, confirming its adaptability and stability during movement.

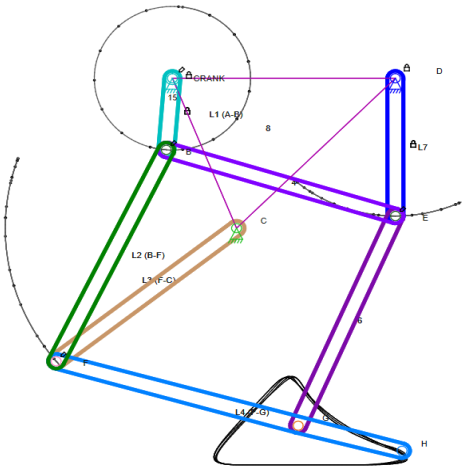

Fig 4. Foot Path Trajectory with a Single Crank Mechanism.

The above Figure 4 highlights repeatability issues in the robot's foot movement while running, particularly evident in the footpath trajectory. As the robot keeps running, its movement becomes less steady due to these problems, especially noticeable when the crank turns from 330 to 45 degrees. This issue, worsening over time with the robot's weight and use, results in a less consistent and balanced path for the robot.

III.i. Motor configuration for robotic trajectory control

Setting up motor 1 (L1): Motor A is configured to exhibit periodic motion, oscillating within a precise range of 1.484 degrees to -1.484 degrees. This range enables accurate angular adjustments in line with our trajectory goals. Configuring motor 2 (L3): Motor C's initial position is approximately 3.02 radians. It is programmed to oscillate around this position, with its movement limited to a maximum of 4.041 radians, periodically returning to its original starting point. This configuration ensures consistent movement aligned with our desired trajectory.

Adjusting motor 3 (L7): Similarly, motor D is initially set to approximately 4.259 radians, and it oscillates within the range of 4.259 radians to 4.979 radians. Its motion revolves around this starting point, aligning with the trajectory requirements.

III.ii. Integrated control systems for synchronized motor trajectories

To achieve synchronized motor trajectories, the set points of the PID controller are strategically calculated to direct the motors toward their respective desired set points. The controlled output, represented by, signifies the adjustment enacted by the PID controller to propel the motor towards the set point. This is mathematically expressed as:

$$u(t) = K_p e(t) + K_i \int e\,(t)dt + K_d \frac{d}{dt} e(t) \qquad (1)$$

Where:

$K_p e(t)$ is the proportional term, which provides a control action proportional to the current error.

$K_i \int e\,(t)dt$ is the integral term, which accounts for the accumulation of past errors and integrates them over time.

$K_d \frac{d}{dt} e(t)$ the derivative term, which predicts the future trend of the error by calculating its rate of change.

The coefficients $K_p, K_i\ and\ K_d$ are the gains for the proportional, integral, and derivative terms, and the error signal $e(t)$ is defined as the difference between the desired set point and the motor's actual position.

III.ii.a. Motor control setup

The configuration of motor control is essential to achieving precise movement patterns. Each motor is assigned a specific desired trajectory set point, which is essential for synchronizing movements.

The desired trajectory set point of motor 1, denoted as $SP_1(t)$, varies sinusoidally between 1.484 and -1.484 radians. The PID control equation governing motor 1 is defined by:

$$u_1(t) = K_{p1} e_1(t) + K_{i1} \int_0^t e_1\,(\tau)dt + K_{d1} \frac{de_1(t)}{dt} \quad (2)$$

For motor 2, the set point SP2(t) oscillates between 3.02 and 4.041 radians. The PID control equation for motor 2 is similarly structured:

$$u_2(t) = K_{p2} e_2(t) + K_{i2} \int_0^t e_2\,(\tau)dt + K_{d2} \frac{de_2(t)}{dt} \quad (3)$$

Here, the control system dynamically adapts motor 2 response to align with the fluctuating setpoint trajectory.

The trajectory for motor 3, $SP_3(t)$, exhibits oscillations between 4.259 and 4.979 radians. The PID formula for this motor is given by:

$$u_3(t) = K_{p3} e_3(t) + K_{i3} \int_0^t e_3\,(\tau)dt + K_{d3} \frac{de_3(t)}{dt} \quad (4)$$

This ensures that motor 3 movement is continuously corrected to follow its desired trajectory path, thereby ensuring that each motor follows its respective trajectory accurately and efficiently.

III.ii.b. Calculation of current error

Accurate motor control depends on the precise calculation of the current error, $e_1(t)$, is the difference between the motor's desired trajectory set point, $SP_1(t)$, and its actual position, $P_1(t)$ at any given time. The current error is given by:

$$e_1(t) = SP_1\ (t) - P_1(t) \quad (5)$$

This error is critical for the PID controller to fine-tune the motor output, ensuring it adheres closely to the intended trajectory.

III.iii.c. Calculation of error derivatives

The derivative of the error $\frac{de_1(t)}{dt}$, is the rate of change of the error over time. For error measurements taken at discrete time intervals, the backward difference method is utilized for calculation.

$$\frac{de_1(t)}{dt} = \frac{e_1(t)-e_1(t-1)}{\Delta t} \tag{6}$$

Here, Δt is the time step between the measurements.

III.ii.d. Calculation of error integral

The integral of the error $\int_0^t e_1\ (T)dt$ serves to accumulate the error over time. Using the trapezoidal rule for numerical integration with the constant step time Δt, the integral is the sum of all past errors, each error multiplied by Δt.

$$\int_0^t e_1\ (\tau)d\tau \approx \sum \frac{e_1(t)+e_1(t-1)}{\Delta t} \cdot \Delta t \tag{7}$$

Subsequently, the control signal $u_1(t)$ is determined using the PID equation

$$u_1(t) = K_{p1}.e_1(t) + K_{i1} \cdot \int_0^t e_1\ (\tau)dt + K_{d1} \cdot \frac{de_1(t)}{dt}$$

This equation adjusts the motor output to reach the desired position by incorporating the proportional, integral, and derivative responses to the error.

III.ii.e. Control circuit

Figure 5 presents a PID control system that manages three servo motors to achieve precise robotic movements. An individual PID controller, which utilizes proportional, integral, and derivative feedback, actively governs each motor to adjust its angle. Servo drives tailor these control signals to the specific inertia and damping characteristics unique to each motor. The system is designed around a second-order dynamic model, which is crucial for quick and accurate responsiveness. Real-time feedback loops are instrumental in providing essential positional information, enabling immediate error correction, and thus preserving the accuracy of the motor trajectories. An onboard gyroscope detects mechanical vibrations, permitting the system to proactively adjust and maintain the robot's stability during operation. This setup demonstrates an integrated approach to achieving precise and adaptable robotic control.

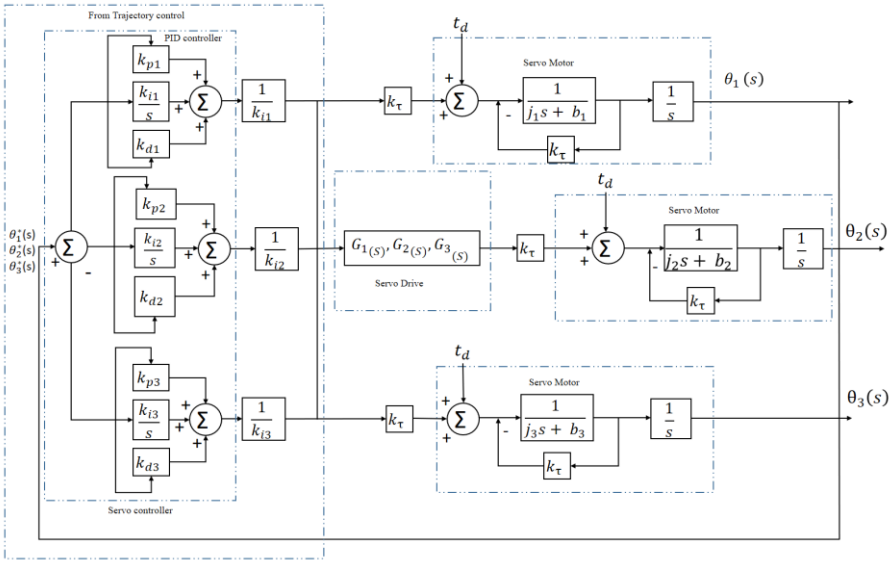

Fig. 5. Three-Channel PID-Controlled Servo Motor Drive System.

III.iii. Torque and power requirements

For a walking leg mechanism, calculating the torque and power begins with assessing the mass and the moment of inertia. The moment of inertia is pivotal in predicting the leg's dynamics and is given by:

$$I_{total} = \sum_{i=1}^{n} \frac{1}{3} m_i l_i^2 \quad (8)$$

Here represents the mass moment of inertia of the mechanism. The variable m_i is the mass of the i^{th} link, and l_i is the length of the i^{th} link. The variable n stands for the number of links in the walking mechanism. The total moment of inertia for the walking leg mechanism is calculated as follows: Based on this value, the torque required for each actuator to provide the kinematic power necessary for the robot leg is specified for three motors:

Motor 1 requires a torque of 1.83×10^{-5} Nm
Motor 2 requires a torque of 3.71×10^{-4} Nm
Motor 3 requires a torque of 3.83×10^{-4} Nm

The power requirement of these motors at 5 rpm are:

Motor 1: 9.53×10^{-5} Nm
Motor 2: 1.94×10^{-4} Nm
Motor 3: 2.01×10^{-4} Nm

These torque values represent the peak torque that would be necessary at the highest angular acceleration for each motor, accounting for the distribution of mass across the links. The power required by the motors to achieve their respective peak torques at 5

rpm can vary depending on external loads, friction, operational speed, and other environmental factors. Additionally, experimental data, such as the graphs in Figure 13, suggest that improvements in speed are possible while maintaining system balance. This indicates that even with a balanced system, there is potential for optimizing speed, likely through adjustments in the mechanism's design or control system.

III.iv. Control process

The control system diagram in Figure 6 for a robot illustrates a feedback loop where positional data informs the computation of movement errors. A PID microcontroller corrects these errors by controlling servo motors through drivers. Optical encoders on the motors furnish feedback, facilitating exact trajectory tracking. This precision allows the robot to perform complex tasks with high accuracy.

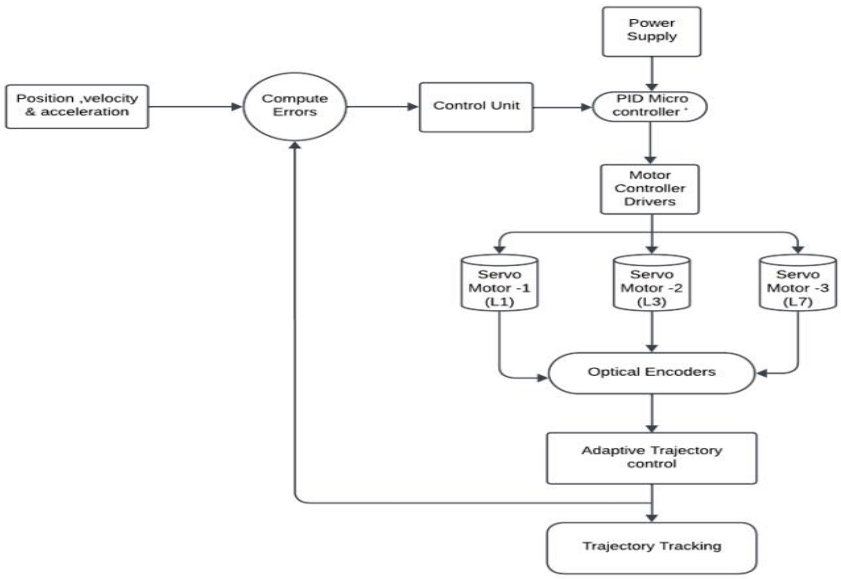

Fig. 6. Control System Architecture for Adaptive Trajectory Tracking in Multi-Legged Robot tracking.

III.v. The reconfigured leg controller design

The control system in Figure 7 utilizes the STM32F051 microcontroller to operate a Peaucellier-Lipkin mechanism. This microcontroller, operating at a frequency of 48 MHz, is chosen for its balance of performance, cost-effectiveness, and low power consumption. It is equipped with eight timer modules, three of which are specifically allocated for decoding signals from quadrature incremental rotary encoders. The encoders deliver precise position feedback for three motors, each set to operate within certain ranges: Motor A at ±1.484 degrees, Motor C near 3.02 radians, and Motor D from 4.259 to 4.979 radians. The STM32F051 employs PID control loops to dynamically adjust these motors, ensuring they remain within their designated ranges. The other timer modules are utilized to generate pulse width modulation (PWM)

signals, which directly control up to five linear RC servos. This configuration obviates the need for extra external drivers, thus simplifying the system. Additionally, the setup includes an ESP32 servo driver expansion board, which adds WiFi and Bluetooth capabilities for remote operation and monitoring. The MPU-9250 sensor module, comprising a gyroscope, accelerometer, and magnetometer, significantly enhances the system by offering comprehensive motion tracking. This sensor is crucial for real-time motion correction and stabilization, thereby improving the accuracy and control of the system. Altogether, this arrangement demonstrates an advanced approach to robotic control, merging precision mechanics with state-of-the-art communication and tracking technologies.

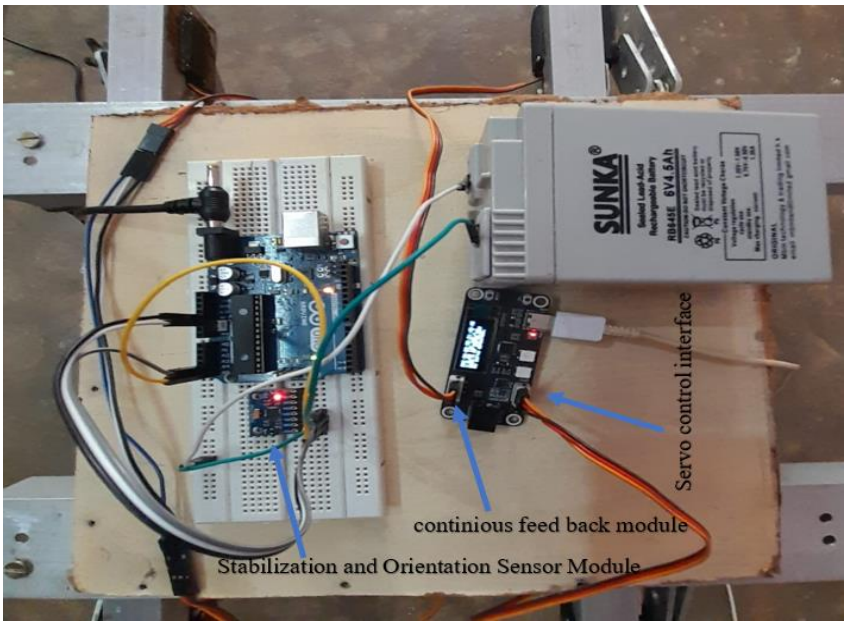

Fig. 7. Integrated Control System for Modified Peaucellier-Lipkin Mechanism with Advanced Motion Tracking.

IV. Experimental Validations

Figure 8 shows the footpath trajectory created by a mechanism controlled at three specific points: A, D, and C. This multi-point control mechanism overcomes the limitations observed in Fig. 4, which depicts a single-crank system. The trajectory not only exhibits high repeatability but also maintains exceptional precision, representing a significant improvement over the previous model. The advanced design effectively mitigates the issues related to the self-weight impact that were evident in the single crank mechanism, particularly during the critical transition from 330 to 45 degrees of the crank angle. This improved structure ensures consistently accurate trajectories during both the peak of the transfer phase and the start of the stance phase. The

enhanced repeatability and accuracy have been verified through meticulous readings obtained from optical encoders.

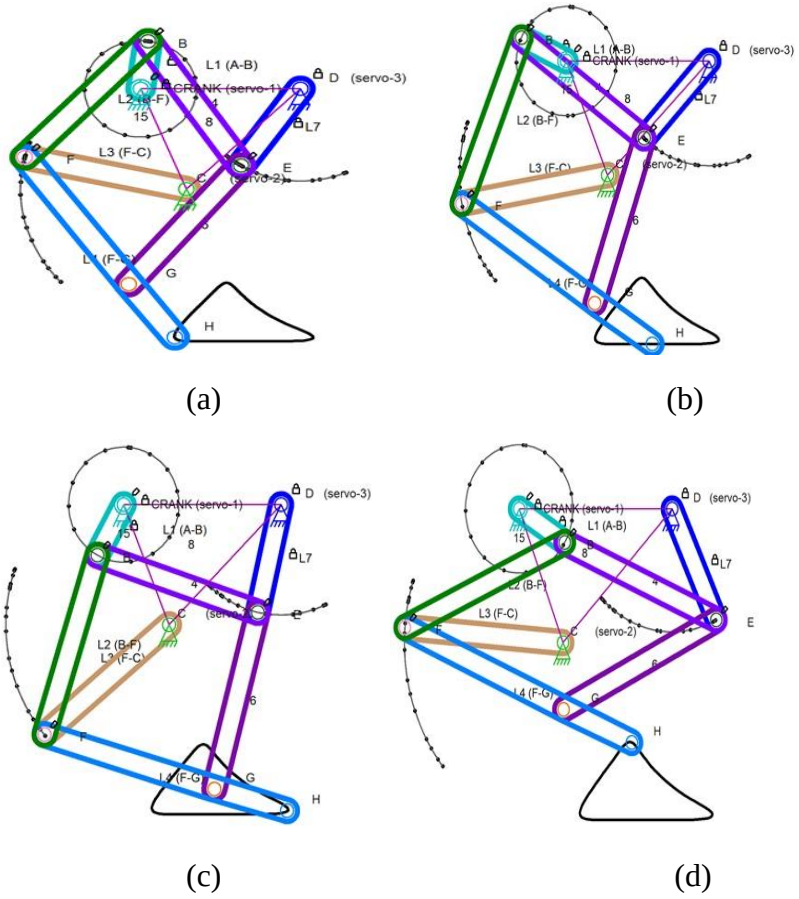

Fig. 8. Foot Trajectory of a Modified Walking Mechanism with Servo Actuation.

IV.i. Integrated Kinematic Analysis of Multi-Motor Systems

Figure 9 displays the simulation results by displaying nine individual line plots, organized in a 3x3 grid. Each row represents one of three motors, with each column showing a different kinematic variable: position, velocity, and acceleration. These plots cover a 24-second interval at 5 RPM, illustrating sinusoidal variations for each motor. The plots use thicker lines for enhanced clarity and effectively demonstrate the periodic kinematic behaviour of each motor within the specified time frame.

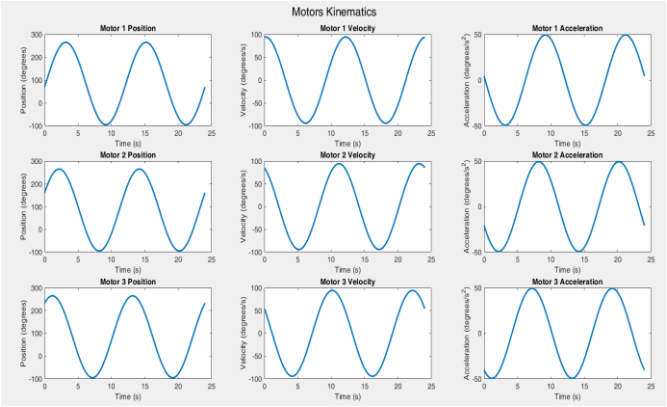

Fig. 9. Motor Kinematic Profiles.

Simulation results are presented in Figure 10, which offers an integrated view of the kinematic behavior of motors 1, 2, and 3 by merging their velocity and acceleration profiles into a single coherent plot. This plot provides a comprehensive graphical representation of the kinematics of the three motors, showcasing how their positions, velocities, and accelerations vary over time. Such analysis is particularly useful for optimizing and understanding the behavior of complex mechanical systems; moreover, the detailed kinematic analysis it affords offers valuable insights for evaluating and refining mechanical operations across various applications.

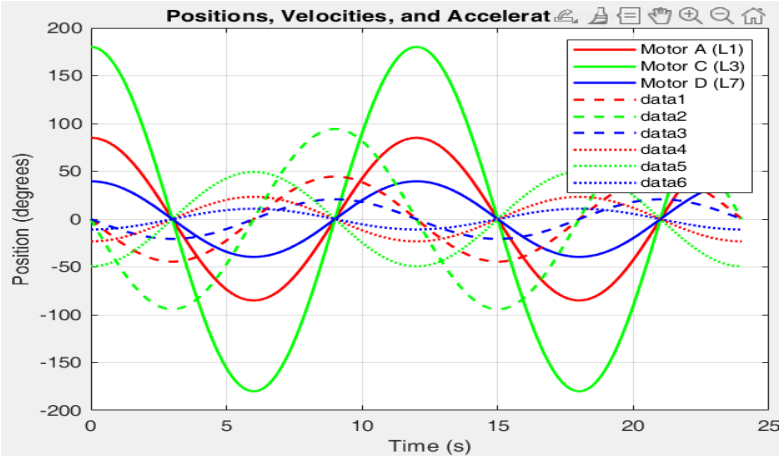

Fig. 10. Composite Velocity and Acceleration Curves of Motors.

The final output is a graphical representation, as shown in Figure 11, of the paths of three mechanical links (L1, L3, and L7) and their angular displacements as functions of time. These plots are useful for visualizing the motion of mechanical links and understanding their angular displacements with respect to time, making them a valuable tool for engineering and kinematic analysis.

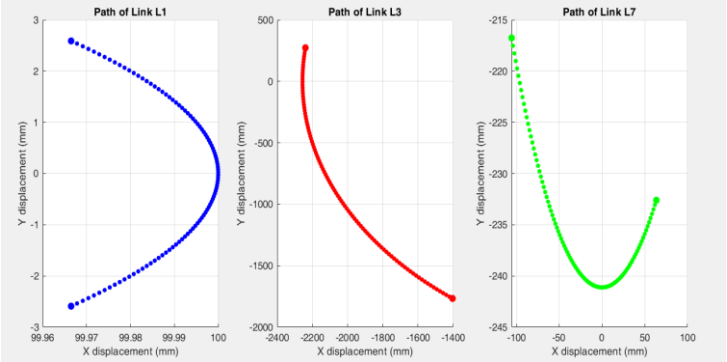

Fig. 11. Linear Displacements of Three Links.

IV.ii. Evaluation of Robot Locomotion: Insights from Gyroscopic Data Experimentation

The experiments conducted on a consistently paced robot operating on flat terrain yielded varied gyroscopic readings. The three-axis gyroscope, positioned on top of the robot, provided critical data during tests of a single motor control system for each leg. The data captured from the gyroscope reflected deflections along three axes: Value 1 as the x-axis, Value 2 as the y-axis, and Value 3 as the z-axis. As shown in Figure 12, the readings exhibited greater amplitudes along all three axes when the robot operated without additional control inputs. This suggests more pronounced shifts in orientation, potentially signaling instability or gait inefficiencies. These insights will be crucial for refining the control systems in future iterations.

Fig. 12. Single crank locomotion gyro readings.

By incorporating three control points, as shown in Figure 3 (A, C, and D), the robot was tested on flat terrain. The gyroscopic readings, depicted in Figure 13, showed a reduced amplitude in sensor outputs across all axes, indicating less variation in the

robot's orientation. These findings suggest improved stability and a more consistent walking pattern, highlighting the effectiveness of the applied control measures. The graph clearly illustrates how the implemented control system successfully minimized instability, leading to smoother movements and a reduction in shifts or irregularities in the robot's gait.

Fig. 13. Multi Controlled Points Locomotion Gyro Readings.

IV.iii. Assembled Model with Different Walking Gaits

The CAD images presented in Figures 14-17 illustrate various walking gaits of a robot, featuring series, parallel, and assembled. These visualizations are valuable for demonstrating robotic gait patterns and are suitable for educational or engineering purposes. They effectively emphasize the design and functionality of the robot's locomotion system.

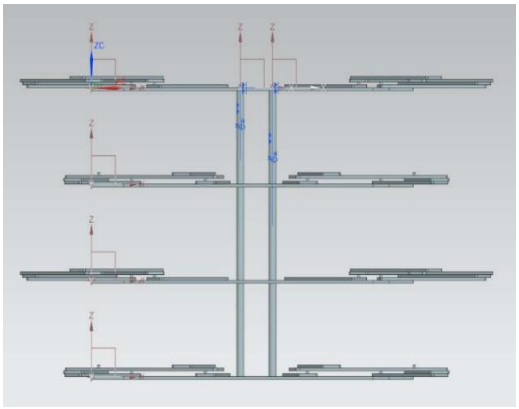

Fig. 14. Parallel Walking Gait.

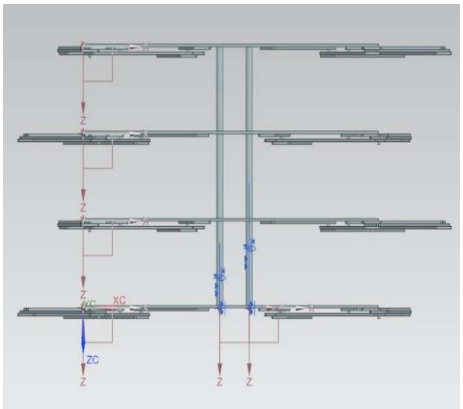

Fig. 15. Series Walking Gait.

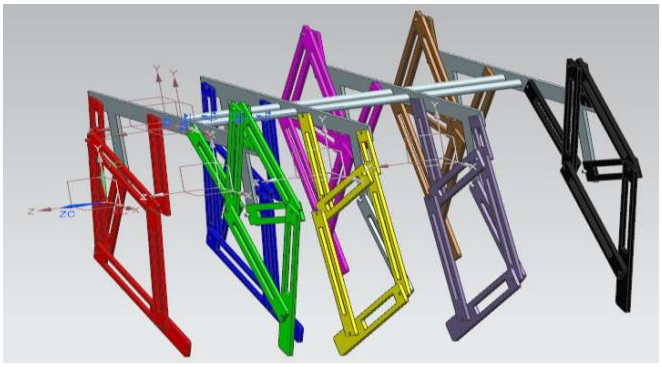

Fig 16. Assembled model

IV.i. Robot Environmental Adaptability Trial

To conduct a field test of the robot, the modified control mechanism will be executed across various environments to ensure successful adaptation and performance. The test will provide a glimpse into the robot's versatility in handling diverse and potentially challenging conditions.

Fig. 17. Field Test of Multi-Legged Robot on Grass Terrain

Fig. 18. Field Test of Multi-Legged Robot on irregular Terrain

V. Conclusion

In this paper, we present a reconfigurable design accompanied by a fully realized prototype of a robot that utilizes a modified Peaucellier-Lipkin mechanism controlled by three servo motors. This advanced design improves the robot's walking

stability. The application of PID control serves as an intelligent automatic adjustment, enhancing the robot's movement consistency over time, which is crucial for its effective operation across diverse environments. Moreover, the system enables the robot to swiftly alter its walking pattern, a feature that is particularly useful for maneuvering through different terrains. The integration of PID control with sensor feedback ensures precise and flexible motion, equipping the robot to smoothly adapt to new situations. The gyro readings also contribute to this level of control and adaptability, making the robot versatile and dependable, suitable for both everyday applications and more demanding tasks. This innovation represents a significant advance in robotic mobility, bringing robots closer to emulating the complex movements of living organisms.

VI. Future scope

Future enhancements to the robot will focus on reducing dependency on a single crank for improved self-adjustment, distributing control with new actuators for better adaptability and efficiency, and reinforcing the design to prevent mechanical failures and extend the robot's operational capabilities in varied settings. The paper indicates that advancing PID tuning and integrating AI could create smarter, more energy-efficient control systems, enhancing the robot's ability to adapt to different terrains like legged animals.

Conflict of Interest:

The author confirms that there are no conflicts of interest related to this paper.

Reference

I. Alexeev, L., Dobra, A., & Lovasz, E.: "Walking Robot with Modified Jansen Linkage." In Machine and Industrial Design in Mechanical Engineering, Mechanisms and Machine Science 109, Springer Nature Switzerland, 2022, Ch. 58, p. 577. 10.1007/978-3-030-88465-9_58

II. Bhavsar, Keval, Dharmik Gohel, Pranav Darji, Jitendra Modi, and Umang Parmar.: 'Kinematic Analysis of Theo Jansen Mechanism-Based Eight-Leg Robot'. In Advances in Fluid Mechanics and Solid Mechanics: Proceedings of the 63rd Congress of ISTAM 2018, pp. 75-82. Singapore: Springer Singapore, 2020. 10.1007/978-981-32-9971-9_30

III. Chen, X., Wang, L. Q., Ye, X. F., Wang, G., & Wang, H. L.: "Prototype Development and Gait Planning of Biologically Inspired Multi-Legged Crablike Robot." Mechatronics, 2013, 23(4), pp. 429-444. 10.1016/j.mechatronics.2013.03.006

IV. Chwila, S., Zawiski, R., and Babiarz, A.: 'Developing and Implementation of the Walking Robot Control System'. In Man-Machine Interactions 3, Springer International Publishing, pp. 97-105, 2014. 10.1007/978-3-319-02309-0_10

V. Desai, Shivamanappa G., Anandkumar R. Annigeri, and A. TimmanaGouda.: 'Analysis of a New Single Degree-of-Freedom Eight Link Leg Mechanism for Walking Machine'. Mechanism and Machine Theory, Vol. 140, pp. 747-764, 2019. 10.1016/j.mechmachtheory.2019.06.002

VI. Gao, H., Kareem, A., Jawarneh, M., Ofori, I., Raffik, R., and Kishore, K.H.: '[Retracted] Metaheuristics Based Modeling and Simulation Analysis of New Integrated Mechanized Operation Solution and Position Servo System'. Mathematical Problems in Engineering, 2022(1), p. 1466775. 10.1155/2022/1466775

VII. Ghassaei, Amanda, Professors Phil Choi, and Dwight Whitaker.: "The Design and Optimization of a Crank-Based Leg Mechanism." Pomona, USA (2011).

VIII. Giesbrecht, Daniel. Design and Optimization of a One-Degree-of-Freedom Eight-Bar Leg Mechanism for a Walking Machine. MS thesis, 2010. http://hdl.handle.net/1993/3922

IX. Haidar, A. M., C. Benachaiba & M. Zahir.: "Software Interfacing of Servo Motor with Microcontroller." Journal of Electrical Systems, vol. 9, (1) pp. 84-99, 2013. https://ro.uow.edu.au/eispapers/468/

X. Janson, T. The Great Pretender. Uitgeverij, 2007.

XI. Jaichandar, K., Mohan Rajesh, E., Martínez-García, E., and Le Tan-Phuc.: 'Trajectory Generation and Stability Analysis for Reconfigurable Klann Mechanism Based Walking Robot'. Robotics, Vol. 5, No. 3, pp. 1-12, 2016. https://doi.org/10.3390/robotics5030013

XII. Jaichandar, K., Rajesh Elara M., Martínez-García E., & Tan-Phuc L.: "Synthesizing Reconfigurable Foot Traces Using a Klann Mechanism." Robotica, 35(1), 2015. Cambridge University Press. https://doi.org/10.1017/S0263574715000089

XIII. Kajita, Shuuji, and Bernard Espiau.: 'Legged Robot'. Springer Handbook of Robotics. Berlin/Heidelberg, Germany: Springer, pp. 361-389, 2008.

XIV. Khaled, Nassim.: "Acceleration Based Approach for Position Control." IOP Conference Series: Materials Science and Engineering, Vol. 717, No. 1, IOP Publishing, 2020. 10.1088/1757-899X/717/1/012020

XV. Kim, D.H.: 'Design and Tuning Approach of 3-DOF Emotion Intelligent PID (3-DOF-PID) Controller'. In 2012 Sixth UKSim/AMSS European Symposium on Computer Modeling and Simulation, IEEE, pp. 74-77, November 2012. https://doi.org/10.1109/EMS.2012.93

XVI. Klann, J.C.: Patent No. 6.260.862, USA, 2001. https://patents.google.com/patent/US6260862B1/en

XVII. Krishnamurthy, Balachandar, Sabari Senbagarajan, and Lokesh Mahendran.: 'Design and Fabrication of Spider Bot'. AIP Conference Proceedings, Vol. 2946, No. 1, AIP Publishing, pp. 1-5, 2023. https://doi.org/10.1063/5.0178024

XVIII. McCarthy, J. M., and Kevin Chen.: Design of Mechanical Walking Robots. MDA, Press, 2021. https://www.google.co.in/books/edition/Design_of_Mechanical_Walking_Robots/-gfozgEACAAJ?hl=te

XIX. Papoutsidakis, M., Chatzopoulos, A., Symeonaki, E., and Tseles, D.: 'Methodology of PID Control – A Case Study for Servomotors'. International Journal of Computer Applications, Vol. 179, No. 30, pp. 30-33, 2018. 10.5120/ijca2018916689

XX. Sheba, J.K., Martínez-García, E., Elara, M.R., and Tan-Phuc, L.: 'Design and Evaluation of Reconfigurable Klann Mechanism Based Four-Legged Walking Robot'. In 2015 10th International Conference on Information, Communications and Signal Processing (ICICS), IEEE, pp. 1-5, December 2015. 10.1109/ICICS.2015.7459939

XXI. Sun, Jiefeng, and Jianguo Zhao.: 'An Adaptive Walking Robot with Reconfigurable Mechanisms Using Shape Morphing Joints'. IEEE Robotics and Automation Letters, Vol. 4, No. 2, pp. 724-731, 2019. 10.3390/robotics5030013

XXII. Sutyasadi, P., and Parnichkun, M.: 'Gait Tracking Control of Quadruped Robot Using Differential Evolution Based Structure Specified Mixed Sensitivity H∞ Robust Control'. Journal of Control Science and Engineering, 2016(1), p. 8760215, 2016. 10.1155/2016/8760215

XXIII. Vanitha, U., Premalatha, M., Nithinkumar, S., and Vijayaganapathy, S.: 'Mechanical Spider Using Klann Mechanism'. Scholarly Journal of Engineering and Technology, Vol. 3, No. 9, pp. 737-740, December 2015. chrome-extension://efaidnbmnnnibpcajpcglclefindmkaj/https://saspublishers.com/media/articles/SJET39737-740.pdf

XXIV. Visioli, Antonio. Practical PID Control. Springer Science & Business Media, 2006. https://www.google.co.in/books/edition/Practical_PID_Control/ymyAY01bEe0C?hl=te&gbpv=0

XXV. Zielinska, Teresa.: "Development of Walking Machines; Historical Perspective." International Symposium on History of Machines and Mechanisms: Proceedings HMM2004. Springer Netherlands, 2004. 10.1016/S0957-4158(01)00017-4